Tree-level yield estimation using UAV-based vegetation indices and plant physiology-informed machine learning

Haoyu Niu[1], Dong Wang[2], Reza Ehsani[3], and YangQuan Chen[4]

***Abstract*— Estimating the yield of trees is important to improve orchard management and production. Usually, farmers need to estimate the yield of trees at the early growing stage for field management. However, methods to predict the yield at the individual tree level are currently not available because of the complexity and variability of each tree. Thus, in this article, the authors evaluated the performance of an unmanned aerial vehicle (UAV)-based remote sensing system and machine learning (ML) approaches for yield estimation. A multispectral camera was mounted on the UAV platform to acquire high-resolution images. Eight features were extracted from the UAV imagery, including normalized difference vegetation index (NDVI), green normalized vegetation index (GNDVI), red-edge normalized difference vegetation index (NDVIre), red-edge triangulated vegetation index (RTVIcore), individual tree canopy size, the modified triangular vegetation index (MTVI2), the chlorophyll index-green (CIg), and the chlorophyll index-rededge (CIre). Then, plant physiology-informed machine learning (PPIML) algorithms were applied with the extracted features to predict the yield at the individual tree level. Results showed that the decision tree classifier had the best prediction performance, with an accuracy of 85%.**

I. INTRODUCTION

54 pt
0.75 in
19.1 mm

The yield of field and woody crops is usually determined by their genotype and environmental conditions, such as soil physical and chemical properties, irrigation management, weather conditions, etc., making the yield prediction complicated and inaccurate [1], [2]. Thus, many researchers have been working on the yield prediction using a plethora of approaches [3], [4], [5], [6], [7]. For example, Zhang *et al.* [3] developed statistical models using the stochastic gradient boosting method for early and mid-season yield prediction of almond in the central valley of California. Multiple variables were extracted from the remote sensing images, such as canopy cover percentage (CCP) and vegetation indices (VIs). Research results demonstrated the potential of automatic almond yield prediction at the individual orchard level. In [8], Yang *et al.* estimated the corn yield by using the hyperspectral imagery and convolutional neural networks (CNNs). Results showed that the spectral and color image-based integrated CNN model has a classification accuracy of 75% for corn yield prediction.

[1]Haoyu Niu is a Ph.D. candidate at University of California, Merced, 5200 Lake Rd, Merced, CA 95340, USA hniu2@ucmerced.edu
[2]Dr. Dong Wang is a Lead Reseacher at USDA-ARS Water Management Research Unit, San Joaquin Valley Agricultural Sciences Center,Parlier, CA dong.wang@ars.usda.gov
[3]Prof. Reza Ehsani is a professor at University of California, Merced, 5200 Lake Rd, Merced, CA 95340, USA rehsani@ucmerced.edu
[4]Prof. YangQuan Chen is a professor at University of California, Merced, 5200 Lake Rd, Merced, CA 95340, USA ychen53@ucmerced.edu

Recently, unmanned aerial vehicles (UAVs) and lightweight payloads have been used as a reliable remote sensing platform by many researchers to monitor the crop status temporally and spatially [9], [10], [11], [12]. Equipped with lightweight payloads, such as RGB camera, multispectral camera, and thermal camera, UAV-based remote sensing system can provide low-cost and high-resolution images for data analysis. For example, in [4], Yang *et al.* proposed an efficient CNN for rice grain yield estimation. A fixed-wing UAV was adopted to collect RGB and multispectral images to derive the vegetation indices. Results showed that the CNNs trained by RGB and multispectral imagery had better performance than the VIs-based regression model. In [5], Stateras *et al.* defined the geometry of olive tree configurations and developed a forecasting model of annual production in a non-linear olive grove. Digital terrain model (DTM) and digital surface model (DSM) were generated with high-resolution multispectral imagery. Results showed that the forecasting model could predict the olive yield in kilograms per tree.

However, few studies have investigated the correlation between the tree canopy characteristics and yield prediction at the individual tree level. Thus, this article aims to estimate the pomegranate tree yield with ten different tree canopy characteristics, which are normalized difference vegetation index (NDVI), green normalized vegetation index (GNDVI), red-edge normalized difference vegetation index (NDVIre), red-edge triangulated vegetation index (RTVIcore), canopy size, canopy temperature, irrigation level, the modified triangular vegetation index (MTVI2), the chlorophyll index-green (CIg) and the chlorophyll index-rededge (CIre). For example, the NDVI has been commonly used for vegetation monitoring, such as water stress detection [13], crop yield assessment [14], and evapotranspiration (ET) estimation [15]. The value of NDVI is a standardized method to measure healthy vegetation. When the NDVI is high, it indicates that the vegetation has a higher level of photosynthesis. In [1], Feng *et al.* demonstrated that the NDVI and yield had a Pearson correlation coefficient of 0.80. The GNDVI and yield had a correlation of 0.53.

54 pt
0.75 in
19.1 mm

The **objectives of this article** were: 1.) Estimated the yield using UAV-based vegetation indices. 2.) Demonstrated the performance of several ML algorithms on tree-level yield prediction. The **major contribution of this article** was: 1. Developed a reliable tree-level yield prediction method using UAV-based high-resolution multispectral images and ML algorithms. Section II introduced the materials and methods being used for UAV-based yield prediction. Results

and discussion were presented in Section III. In Section IV, the authors drew the conclusive remarks.

II. MATERIAL AND METHODS

A. Experimental Field and Ground Data Collection

This study was conducted in a pomegranate research field at the USDA-ARS, San Joaquin Valley Agricultural Sciences Center (36.594 °N, 119.512 °W), Parlier, California, 93648, USA. The soil types are a Hanford fine sandy loam (coarse-loamy, mixed, thermic Typic Xerorthents). The San Joaquin Valley has a Mediterranean climate with hot and dry summers. Rainfall is insignificant during the growing season, and irrigation is the only source of water for pomegranate growth [16]. Pomegranate (Punica granatum L., cv 'Wonderful') was planted in 2010 with a 5 m spacing between rows and a 2.75 m within-row tree spacing in a 1.3 ha field [17]. There were five yield sampling trees in each block, 80 sampling trees in total, marked with red labels in Fig. 1.

B. UAV Platform and Imagery Data Acquisition

The UAV-based remote sensing system consisted of a UAV platform, called "Hover", and a multispectral camera (Rededge M, Micasense, Seattle, WA, USA). The Rededge M has five different bands, which are Blue (B, 475 nm), Green (G, 560 nm), Red (R, 668 nm), Red Edge (RedEdge, 717 nm), and Near Infrared (NIR, 840 nm). With a Downwelling Light Sensor (DLS), a 5-band light sensor that connects to the camera, the Rededge M can measure the ambient light during a flight mission for each of the five bands. Then, it can record the light information in the metadata of the images captured by the camera. After the camera calibration, the information detected by the DLS can be used to correct lighting changes during a flight, such as changes in cloud cover during a UAV flight.

A software Mission Planner was used to design the flight missions. The flight height was designed as 60 m above ground level (AGL). The UAV image overlapping was designed as 75% in forward and 70% sideward to stitch UAV images successfully by Agisoft Metashape (Agisoft LLC., Russia).

C. UAV Image Feature Extraction

1) The Normalized Difference Vegetation Index (NDVI): The NDVI has been commonly used for vegetation monitoring, such as water stress detection [13], crop yield assessment [14], and ET estimation [18]. The value of NDVI is a standardized method to measure healthy vegetation, allowing to generate an image displaying greenness (relative biomass). The NDVI takes advantage of the contrast of the characteristics of two bands, which are the chlorophyll pigment absorptions in the red band (R) and the high reflectivity of plant materials in the near-infrared band (NIR). When the NDVI is high, it indicates that the vegetation has a higher level of photosynthesis. The NDVI is usually calculated by

$$NDVI = \frac{NIR - R}{NIR + R}, \tag{1}$$

where NIR and R are the reflectance of near-infrared and red band, respectively.

2) The Green Normalized Difference Vegetation Index (GNDVI): The GNDVI is commonly used to estimate photo synthetic activity and determine water and nitrogen uptake into the plant canopy [19], [1]. The GNDVI is calculated by

$$GNDVI = \frac{NIR - G}{NIR + G}, \tag{2}$$

where G stands for the reflectance of the green band.

3) The Red-Edge Normalized Difference Vegetation Index (NDVIre): The NDVIre is a method for estimating vegetation health using the red-edge band. The chlorophyll concentration is usually higher at the late stages of plant growth; the NDVIre can then be used to map the within-field variability of nitrogen foliage to help better understand the fertilizer requirements of crops [20], [21]. The NDVIre is calculated by

$$NDVIre = \frac{NIR - RedEdge}{NIR + RedEdge}, \tag{3}$$

where $RedEdge$ is the reflectance of the red-edge band.

4) The Red-Edge Triangulated Vegetation Index (RTVIcore): The RTVIcore is usually used for estimating the leaf area index and biomass [22], [23]. It uses the reflectance in the NIR, RedEdge, and G spectral bands, calculated by

$$RTVIcore = 100(NIR - RedEdge) - 10(NIR - G). \tag{4}$$

5) The Modified Triangular Vegetation Index (MTVI2): The MTVI2 method usually detects the leaf chlorophyll content at the canopy scale, which is relatively insensitive to the leaf area index [24]. MTVI2 uses the reflectance in the G, R and NIR bands, calculated by

$$MTVI2 = \frac{1.5[1.2(NIR - G) - 2.5(R - G)]}{\sqrt{(2NIR + 1)^2 - (6NIR - 5\sqrt{R}) - 0.5}}. \tag{5}$$

6) The Green Chlorophyll Index (CIg): The CIg is for estimating the chlorophyll content in leaves using the ratio of the reflectivity in the NIR and G bands [25], which is calculated by

$$CIg = \frac{NIR}{G - 1}. \tag{6}$$

7) The Red-Edge Chlorophyll Index (CIre): The CIre is for estimating the chlorophyll content in leaves using the ratio of the reflectivity in the NIR and RedEdge bands [25], which is calculated by

$$CIre = \frac{NIR}{RedEdge - 1}. \tag{7}$$

D. The Plant Physiology-informed Machine Learning

Considering the volume, diversity, and complexity of the agricultural dataset, plant physiology-informed machine learning (PPIML) was proposed in this section. The key of this concept is to extract meaningful agricultural information out of the big data to guide stakeholders and researchers to

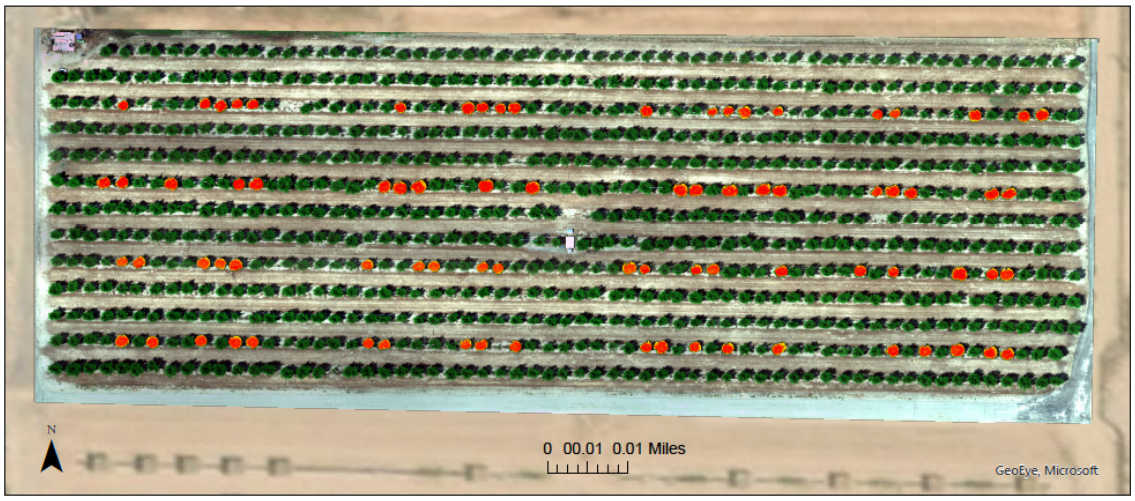

Fig. 1. The pomegranate field was randomly divided into 16 equal blocks, with four replications, to test four irrigation levels. The irrigation volumes are 35%, 50%, 75%, and 100% of ET_c, which was measured by the weighing lysimeter in the field.

make better decisions for agriculture, in which the big data becomes "smart". Instead of training the ML models directly, plant-physiology knowledge will be added into the training process, which helps explain the complexity and model performance. Instead of using the UAV-based image directly, in this article, the authors first extracted the vegetation index information out of the dataset. Then, the vegetation indices were used as input features for the ML algorithms.

Several ML classifiers were adopted to evaluate the performance of pomegranate yield estimation, such as "Random Forest" [26], "AdaBoost" [27], "Nearest Neighbors" [28], and "Decision Tree" [29]. The "Random Forest" classifier is a meta-estimator that fits several decision tree classifiers on various sub-samples of the dataset and adopts averaging to improve the predictive accuracy and control overfitting. An "AdaBoost" classifier is also a meta-estimator that begins by fitting a classifier on the original dataset and then fits additional copies of the classifier on the same dataset but where the weights of incorrectly classified instances are adjusted such that subsequent classifiers focus more on complex cases.

The "Nearest Neighbors" method is to apply a predefined number of training samples closest in the distance to the new point and predict the label from these. The samples can be a constant k-nearest neighbor learning or vary based on the local density of points (radius-based neighbor learning). Despite its simplicity, the nearest neighbor's method has been successfully applied for many research problems, such as the handwritten digits classification. As a non-parametric method, it is often successful in classification situations where the decision boundary is very irregular.

III. Results and Discussion

A. The Pomegranate Yield Performance in 2019

The pomegranate fruit was harvested from 80 sampling trees in 2019. There were four different irrigation levels in the field, 35%, 50%, 75%, and 100% of ET. The authors then calculated the total fruit weight per tree (kg) and drew the boxplot for each irrigation level (Fig. 2). For the 35% irrigation treatment, the total fruit weight per tree was 23.92 kg, which produced the lowest yield. For the 50% irrigation treatment, the total fruit weight per tree was 27.63 kg. For 75% and 100% irrigation treatment, the total fruit weight per tree was 29.84 kg and 34.85 kg, respectively. The pomegranate yield performance at the USDA is consistent with previous research work [17]. Since the authors have the yield data for each sampling tree, machine learning algorithms were used for individual tree level yield estimation with the eight image features mentioned earlier.

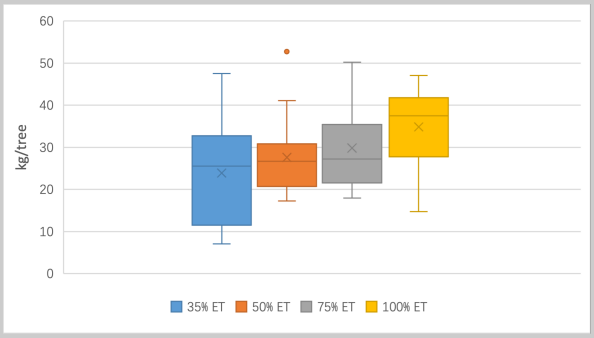

Fig. 2. The pomegranate yield performance at the individual tree level in 2019. For the 35% irrigation treatment, the total fruit weight per tree was 23.92 kg, which produced the lowest yield. For the 50% irrigation treatment, the total fruit weight per tree was 27.63 kg. For 75% and 100% irrigation treatment, the total fruit weight per tree was 29.84 kg and 34.85 kg, respectively.

B. The ML Algorithm Performance on Yield Estimation

The pomegranate yield data (80 sampling trees) was distributed as 75% for training and 25% for testing using the $train\_test\_split$ method. Considering the dataset was

TABLE I
THE "DECISION TREE" PERFORMANCE ON YIELD PREDICTION. "NA" STANDS FOR "NOT AVAILABLE".

Yield prediction	Precision	Recall	F1-score
Low yield	0.92	0.85	0.88
High yield	0.75	0.86	0.80
Accuracy	NA	NA	0.85
Macro avg	0.83	0.85	0.84
Weighted avg	0.86	0.85	0.85

TABLE II
THE PERFORMANCE OF ML METHODS ON YIELD PREDICTION.

Classification methods	Prediction accuracy
"Decision Trees"	**0.85**
"Nearest Neighbors"	0.80
"Support Vector Machine"	0.70
"Random Forest"	0.65
"AdaBoost"	0.80
"Gaussian Process"	0.75
"Gaussian Naive Bayes"	0.60

relatively small, the authors used K-fold cross-validation, splitting the training dataset into K folds, then making predictions and evaluating each fold using an ML model trained on the remaining folds [30]. The classes were defined as low yield and high yield for yield prediction based on a threshold value of 25 kg per tree. For evaluating the trained models, a confusion matrix was used to compare the performances of different classifiers. A confusion matrix was a summary of prediction results on a classification problem. Correct and incorrect predictions were tallied with count values and divided into classes. The confusion matrix provided insight not only into the errors being made by a classifier but, more importantly, the types of errors that were being made. "True label" meant the ground truth of the yield. "Predicted label" identified the individual tree yield predicted by the trained model.

The trained ML classifiers had distinct test performance for individual tree level yield prediction. The "Decision Trees" classifier had the highest accuracy of 0.85. Table I showed the details of the "Decision Trees" method, a non-parametric supervised learning methods commonly adopted for classification problems. For the other classifiers' test performance, the accuracy of the k-nearest neighbor was 0.8. "Support Vector Classification (SVC)" had an accuracy of 0.7. The "Random Forest" had a test accuracy of 0.65. The "AdaBoost", "Gaussian Process", and "Gaussian Naive Bayes" had an accuracy of 0.8, 0.75, and 0.6, respectively. The "Quadratic Discriminant Analysis (QDA)" also had a prediction accuracy of 0.8 (Table II and Fig. 3).

IV. CONCLUSIONS

In this article, the authors performed the individual tree level yield prediction using a UAV-based remote sensing method. The authors collected yield data and the calculated vegetation indices derived from the high-resolution UAV imagery. Then, machine learning algorithms were adopted for the yield prediction classification. The research results showed that the best classification accuracy of yield was 85% when the "Decision Trees" method was being adopted. For the other ML models' test performance, the accuracy of the k-nearest neighbor was 0.8. "Support Vector Classification (SVC)" had an accuracy of 0.7. The "Random Forest" had a test accuracy of 0.65. The "AdaBoost", "Gaussian Process", and "Gaussian Naive Bayes" had an accuracy of 0.8, 0.75, and 0.6, respectively. The "Quadratic Discriminant Analysis (QDA)" also had a prediction accuracy of 0.8. The research results supported the idea that vegetation indices could be used for yield estimation.

ACKNOWLEDGMENT

Thanks go to Stella Zambrzuski for the field measurements. Thanks go to Joshua Ahmed, Allan Murillo, Dong Sen Yan, and Christopher Currier for flying drones.

REFERENCES

[1] A. Feng, J. Zhou, E. D. Vories, K. A. Sudduth, and M. Zhang, "Yield estimation in cotton using UAV-based multi-sensor imagery," *Biosystems Engineering*, vol. 193, pp. 101–114, 2020.
[2] Q. Zaman, A. Schumann, D. Percival, and R. Gordon, "Estimation of wild blueberry fruit yield using digital color photography," *Transactions of the ASABE*, vol. 51, no. 5, pp. 1539–1544, 2008.
[3] Z. Zhang, Y. Jin, B. Chen, and P. Brown, "California almond yield prediction at the orchard level with a machine learning approach," *Frontiers in plant science*, vol. 10, p. 809, 2019.
[4] Q. Yang, L. Shi, J. Han, Y. Zha, and P. Zhu, "Deep convolutional neural networks for rice grain yield estimation at the ripening stage using UAV-based remotely sensed images," *Field Crops Research*, vol. 235, pp. 142–153, 2019.
[5] D. Stateras and D. Kalivas, "Assessment of olive tree canopy characteristics and yield forecast model using high resolution UAV imagery," *Agriculture*, vol. 10, no. 9, p. 385, 2020.
[6] X. Zhang, A. Toudeshki, R. Ehsani, H. Li, W. Zhang, and R. Ma, "Yield estimation of citrus fruit using rapid image processing in natural background," *Smart Agricultural Technology*, p. 100027, 2021.
[7] A. Feng, M. Zhang, K. A. Sudduth, E. D. Vories, and J. Zhou, "Cotton yield estimation from UAV-based plant height," *Transactions of the ASABE*, vol. 62, no. 2, pp. 393–404, 2019.
[8] W. Yang, T. Nigon, Z. Hao, G. D. Paiao, F. G. Fernández, D. Mulla, and C. Yang, "Estimation of corn yield based on hyperspectral imagery and convolutional neural network," *Computers and Electronics in Agriculture*, vol. 184, p. 106092, 2021.
[9] H. Niu, T. Zhao, J. Wei, D. Wang, and Y. Chen, "Reliable tree-level evapotranspiration estimation of pomegranate trees using lysimeter and UAV multispectral imagery," in *2021 IEEE Conference on Technologies for Sustainability (SusTech)*. IEEE, 2021, pp. 1–6.
[10] H. Niu, D. Hollenbeck, T. Zhao, D. Wang, and Y. Chen, "Evapotranspiration estimation with small UAVs in precision agriculture," *Sensors*, vol. 20, no. 22, p. 6427, 2020.
[11] D. Turner, A. Lucieer, Z. Malenovskỳ, D. H. King, and S. A. Robinson, "Spatial co-registration of ultra-high resolution visible, multispectral and thermal images acquired with a micro-UAV over Antarctic moss beds," *Remote Sensing*, vol. 6, no. 5, pp. 4003–4024, 2014.
[12] K. C. Swain, S. J. Thomson, and H. P. Jayasuriya, "Adoption of an unmanned helicopter for low-altitude remote sensing to estimate yield and total biomass of a rice crop," *Transactions of the ASABE*, vol. 53, no. 1, pp. 21–27, 2010.

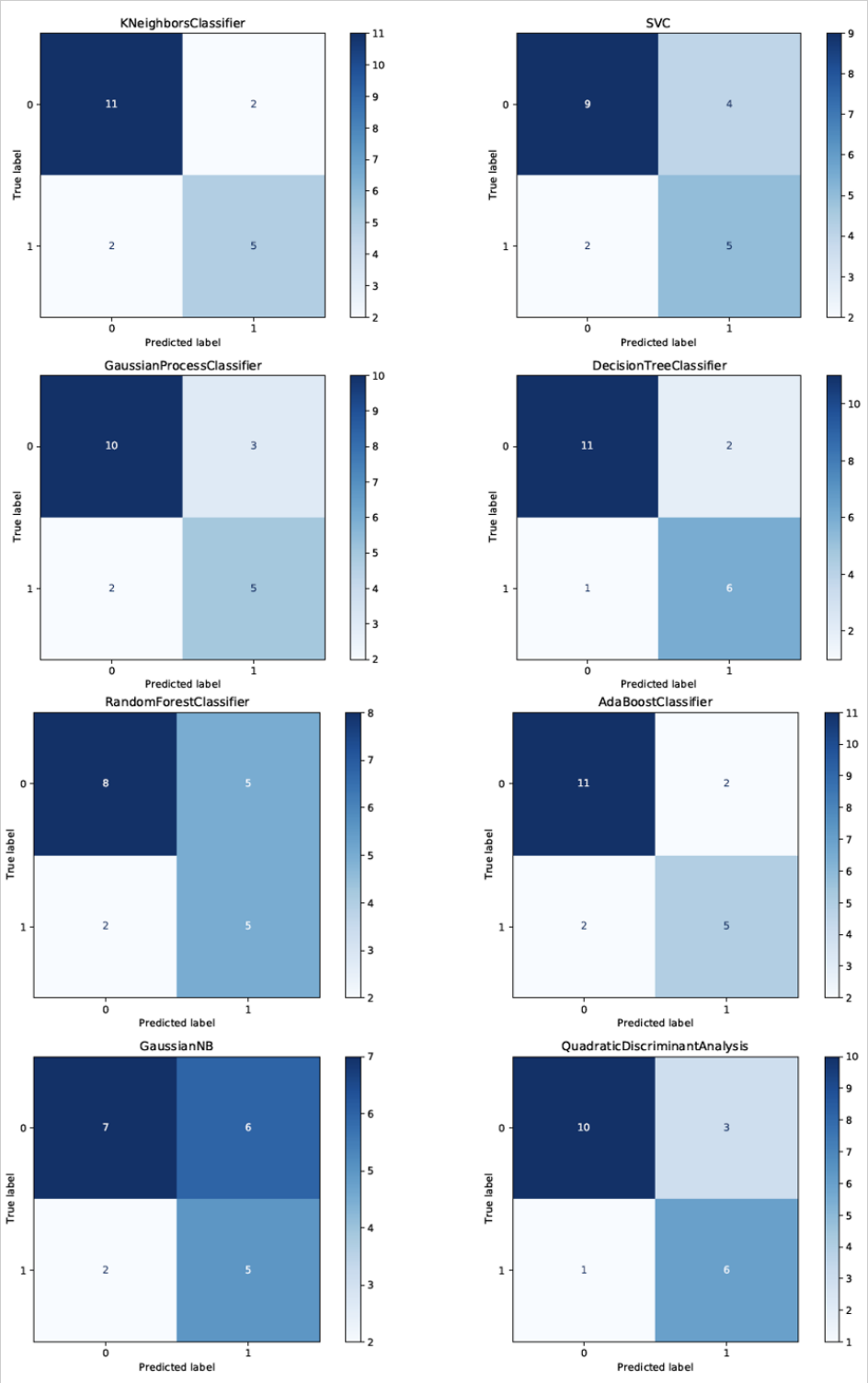

Fig. 3. The comparison of the eight different ML classifiers on individual tree level yield prediction. “True label” meant the ground truth of the yield. “Predicted label” identified the individual tree yield predicted by the trained model. The value 0 meant the low yield; value 1 meant the high yield.

[13] T. Zhao, D. Doll, and Y. Chen, "Better almond water stress monitoring using fractional-order moments of non-normalized difference vegetation index," in *2017 ASABE Annual International Meeting*. American Society of Agricultural and Biological Engineers, 2017, p. 1.
[14] T. Zhao, Z. Wang, Q. Yang, and Y. Chen, "Melon yield prediction using small unmanned aerial vehicles," in *Autonomous Air and Ground Sensing Systems for Agricultural Optimization and Phenotyping II*. International Society for Optics and Photonics, 2017.
[15] H. Niu, D. Wang, and Y. Chen, "Estimating actual crop evapotranspiration using deep stochastic configuration networks model and UAV-based crop coefficients in a pomegranate orchard," in *Autonomous Air and Ground Sensing Systems for Agricultural Optimization and Phenotyping V*. International Society for Optics and Photonics, 2020.
[16] D. Wang, J. Ayars, R. Tirado-Corbala, D. Makus, C. Phene, and R. Phene, "Water and nitrogen management of young and maturing pomegranate trees," in *III International Symposium on Pomegranate and Minor Mediterranean Fruits 1089*, 2013, pp. 395–401.
[17] H. Zhang, D. Wang, J. E. Ayars, and C. J. Phene, "Biophysical response of young pomegranate trees to surface and sub-surface drip irrigation and deficit irrigation," *Irrigation Science*, vol. 35, no. 5, pp. 425–435, 2017.
[18] H. Niu, D. Wang, and Y. Chen, "Estimating crop coefficients using linear and deep stochastic configuration networks models and UAV-based normalized difference vegetation index (NDVI)," in *Proceedings of the 2020 International Conference on Unmanned Aircraft Systems (ICUAS)*. IEEE, 2020, pp. 1485–1490.
[19] K. Yawata, T. Yamamoto, N. Hashimoto, R. Ishida, and H. Yoshikawa, "Mixed model estimation of rice yield based on NDVI and GNDVI using a satellite image," in *Remote Sensing for Agriculture, Ecosystems, and Hydrology XXI*, vol. 11149. International Society for Optics and Photonics, 2019, p. 1114918.
[20] R. A. Schwalbert, T. J. Amado, L. Nieto, S. Varela, G. M. Corassa, T. A. Horbe, C. W. Rice, N. R. Peralta, and I. A. Ciampitti, "Forecasting maize yield at field scale based on high-resolution satellite imagery," *Biosystems engineering*, vol. 171, pp. 179–192, 2018.
[21] O. G. Narin and S. Abdikan, "Monitoring of phenological stage and yield estimation of sunflower plant using Sentinel-2 satellite images," *Geocarto International*, pp. 1–15, 2020.
[22] T. S. Magney, J. U. Eitel, and L. A. Vierling, "Mapping wheat nitrogen uptake from rapideye vegetation indices," *Precision Agriculture*, vol. 18, no. 4, pp. 429–451, 2017.
[23] I. Khosravi and S. K. Alavipanah, "A random forest-based framework for crop mapping using temporal, spectral, textural and polarimetric observations," *International Journal of Remote Sensing*, vol. 40, no. 18, pp. 7221–7251, 2019.
[24] M. Din, W. Zheng, M. Rashid, S. Wang, and Z. Shi, "Evaluating hyperspectral vegetation indices for leaf area index estimation of oryza sativa l. at diverse phenological stages," *Frontiers in plant science*, vol. 8, p. 820, 2017.
[25] Y. Gong, B. Duan, S. Fang, R. Zhu, X. Wu, Y. Ma, and Y. Peng, "Remote estimation of rapeseed yield with unmanned aerial vehicle (UAV) imaging and spectral mixture analysis," *Plant methods*, vol. 14, no. 1, pp. 1–14, 2018.
[26] L. Breiman, "Random forests," *Machine Learning*, vol. 45, no. 1, pp. 5–32, 2001.
[27] D. P. Kingma and J. Ba, "Adam: A method for stochastic optimization," *arXiv preprint arXiv:1412.6980*, 2014.
[28] J. Goldberger, G. E. Hinton, S. Roweis, and R. R. Salakhutdinov, "Neighbourhood components analysis," *Advances in neural information processing systems*, vol. 17, pp. 513–520, 2004.
[29] W.-Y. Loh, "Classification and regression trees," *Wiley Interdisciplinary Reviews: Data Mining and Knowledge Discovery*, vol. 1, no. 1, pp. 14–23, 2011.
[30] A. Géron, *Hands-on Machine Learning with Scikit-Learn, Keras, and TensorFlow: Concepts, Tools, and Techniques to Build Intelligent Systems*. O'Reilly Media, 2019.